Available online at www.sciencedirect.com

jmr&t Journal of Materials Research and Technology

www.jmrt.com.br

Original Article

Dry sliding wear behaviour of single and dual ceramic reinforcements premixed with Al powder in AA6061 matrix

Ponnarengan Hariharasakthisudhan[a,*], *Swaminathan Jose*[b], *Kondal Manisekar*[c]

[a] *Research Scholar - Sathyabama University, Mechanical Engineering Department, National Engineering College, Kovilpatti, Tamil Nadu, India*

[b] *Research Supervisor - Sathyabama University, Mechanical Engineering Department, Loyola-ICAM College of Engineering, Technology, Chennai, Tamil Nadu, India*

[c] *Professor - Mechanical Engineering Department, National Engineering College, Kovilpatti, Tamil Nadu, India*

ARTICLE INFO

Article history:
Received 21 July 2017
Accepted 8 January 2018
Available online 7 March 2018

Keywords:
Metal–matrix composite
Wear testing
Electron microscopy
Surface analysis

ABSTRACT

This work highlighted the preparation of a hybrid of AA6061/Al_2O_3/graphite composite by additionally incorporating Si_3N_4 nanoparticles in the material system. The reinforcements were premixed with Al metal powder to improve their diffusion into the matrix during manufacturing of composites. The composites were manufactured by stir casting method. The pin on disc wear test was carried out as per ASTM G99 standard. Field emission scanning electron microscope (FESEM) and energy dispersive spectroscopy (EDS) analysis were conducted on worn out surface and subsurface of the composite specimens to determine the wear mechanism. From the results, it was found that the wear behaviour of Al powder premixed reinforcement was superior to unmixed reinforcements. The composites with dual ceramic reinforcement have shown lesser wear rate and coefficient of friction than composites with single ceramic reinforcement. Abrasive wear and grain structure refinement just beneath the worn out surface were noted in composites with Si_3N_4 nanoparticles. Single ceramic reinforcement of Al premixed Al_2O_3 was identified with abrasive wear, micro cuts and formation of mechanically mixed layer on the worn out surface. Single ceramic reinforcement of unmixed Al_2O_3 exhibited abrasive wear and severe plastic deformation on worn out surface. Porosity, particle fracture and particle pull out were noticed in the subsurface of the composites with unmixed single ceramic reinforcement of Al_2O_3.

1. Introduction

Inception of using ceramic reinforcement with soft matrix imparted huge development in the field of metal matrix composites (MMC). Tribological behaviour of hard and less dense ceramic particle/fibre dispersed Al based composites were extensively studied by many researchers in micron and

* *Corresponding author.*
E-mail: hariharanmech@nec.edu.in (P. Hariharasakthisudhan).

https://doi.org/10.1016/j.jmrt.2018.01.005

nanoscale as Al MMC has wide range of applications. SiC, Al_2O_3, TiB_2, B_4C, WC are few synthetic ceramics largely used with Al based matrix. Complex metallic alloys (CMA), industrial waste and agro waste were also experimented with aluminium for wear resistance [1].

AA6061 is currently used in construction, automotive, railroad car bodies, and marine structures. Low wear resistance of AA 6061 should be addressed to increase the applications in structural parts as this property directly affects the structural integrity [2]. Al_3O_3 is a hard ceramic particle that improved the tribological properties with various Al alloys. Abrasive wear resistance of A2024 alloy was enhanced by increasing the Al_2O_3 content and size in the composite [3]. Wear resistance of pure Al improved when reinforced with Al_2O_3 and Al_4C_3 at increased sliding speeds [4]. Wear mechanisms of alumina reinforced Al alloys with graphite were observed as decohesion, micro cutting and detachment of material in contact surface followed by crack nucleation and propagation in grain boundaries [5]. Delamination was observed with nano-sized Al_2O_3 reinforced in A2023 matrix [6] and wear rate decreased with increasing content of nano-Al_2O_3 in A6061 matrix [7]. In Order to further improve the wear resistance of Al alloy/Al_2O_3/graphite composite, it is required to focus on controlling the particle pullout and successive crack propagation in grain boundary. Particle pullout is attributed to the inefficient bonding in the matrix/reinforcement interface. Metal particles premixed with nano-sized ceramic reinforcement found to provide better dispersion in controlled stirring time with A356 matrix. Improved interfacial bonding was also noted with metal powder mixed reinforcements in matrix [8]. The Si_3N_4 was found to provide improved fracture toughness with various matrices [9]. The size of the reinforcement particles plays a vital role in deciding the wear and fracture behaviour of the metal matrix composites as it controls the porosity in composites [10].

In this experimental study, it was decided to develop a hybrid of A6061/Al_2O_3/graphite composite by additionally adding Si_3N_4 nanoparticles of average size less than 40 nm. The reinforcements were premixed with Al powder (99.2% purity). It was intended to analyze the effect of metal mixing in reducing the level of particle pullout and to study the effect of Si_3N_4 nanoparticles in the A6061/Al_2O_3/graphite composite to procrastinate the nucleation and propagation of cracks in grain boundaries during wear. Pin on disc wear test was carried out to analyze the tribological behaviour of the composites. The wear behaviour was investigated by varying normal load and sliding speed for constant track length in two categories such as low and high. In case of low category, the normal load was varied as 10 N, 20 N and 30 N for constant sliding speed of 1 m/s and track length of 600 m. In high category, the sliding speed was varied as 1 m/s, 2 m/s and 4 m/s for constant normal load of 40 N and track length of 1000 m.

2. Experimental procedure

2.1. Materials preparation

In the context of developing the composites with A6061 matrix, four different mixes of reinforcements were prepared.

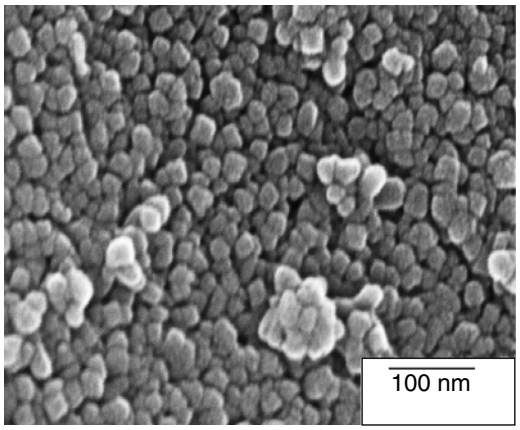

Fig. 1 – Morphology of Si_3N_4 nanoparticles.

Table 1 – Composition of reinforcement.

Reinforcement	Composition
R1	20 wt% Al_2O_3/20 wt% Si_3N_4/55 wt% Al/5 wt% graphite
R2	10 wt% Al_2O_3/30 wt% Si_3N_4/55 wt% Al/5 wt% graphite
R3	45 wt% Al_2O_3/50 wt% Al/5 wt% graphite
R4	95 wt% Al_2O_3/5 wt% graphite

The Si_3N_4 nanoparticles used in this research work was commercially purchased. The Si_3N_4 particles of spherical shape with average size less than 50 nm were purchased from Sigma–Aldrich (now Merck) Chemicals. The purity of the powder was ≥98.5%. The morphology of Si_3N_4 nanoparticle is shown in Fig. 1.

Among all the composites, the amount of reinforcement was 11.5% (120 g). In order to explore the potential of metal powder premixing, the compounds Si_3N_4 and Al_2O_3, were blended with Al powder and graphite particles. The blend was ball milled for 3 h in attrition ball mill with 10 min interval per hour. The premixing process was detailed by the authors elsewhere [11]. The composition details of reinforcement added in each composite are tabulated in Table 1.

Composites were fabricated by stir casting method. A6061 rods of 1050 g were initially melted in the furnace. Molten liquid temperature was maintained at 850 °C. Reinforcements were preheated to the temperature of 150 °C and they were introduced into the molten metal in three stages where each stage of introduction was followed by stirring at low, middle and top of the melt with graphite stirrer. Two minutes of stirring was done at each depth with the stirring speed of 500 rpm. The molten mix was casted as cylindrical rod. The FESEM images of mixed reinforcement 1 are shown in Fig. 2(a), which shows the presence of Al_2O_3 in the form of flakes and other particles and (b) represents the nanoparticles with small clusters. The EDS report is given in Fig. 3. The XRD result of the prepared composite is shown in Fig. 4, which explains the crystalline nature of the composites. The mechanical properties of composites discussed elsewhere are shown in Table 2.

2.2. Wear analysis

Pin on disc wear test was carried out as per ASTM G99 standard at room temperature. Cylindrical composite specimens of

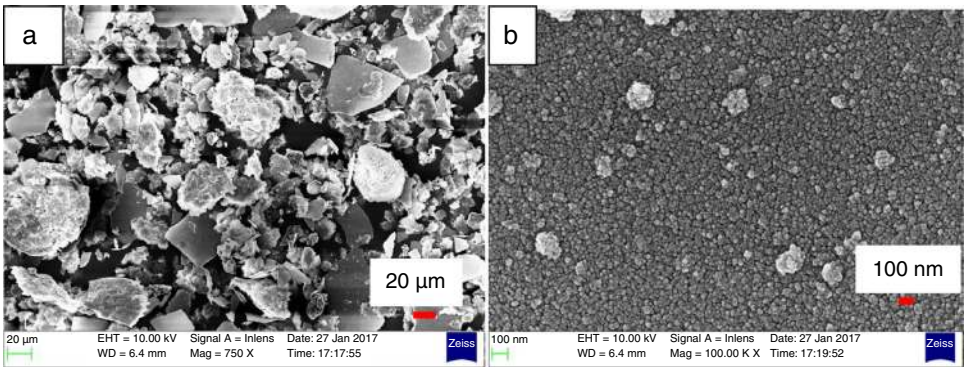

Fig. 2 – SEM images of (a) blended reinforcement R1 and (b) nanoparticles with small clusters in R1.

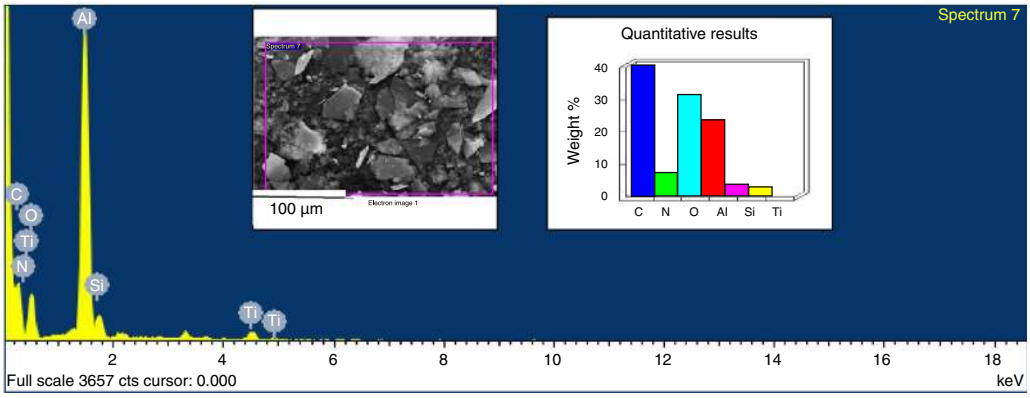

Fig. 3 – EDS report of mixed reinforcement R2 [18].

Table 2 – Mechanical properties of composites.

Composites	Ultimate tensile strength (MPa)	Ultimate compressive strength (MPa)	Vickers hardness (HV)	Ductility (%)
Cast 1(R1)	131.84	292.6	62.2	5
Cast 2 (R2)	153.78	278.49	61.5	8.3
Cast 3 (R3)	96.16	361.74	66.3	2.5
Cast 4 (R4)	44.14	298.2	59.9	1.25

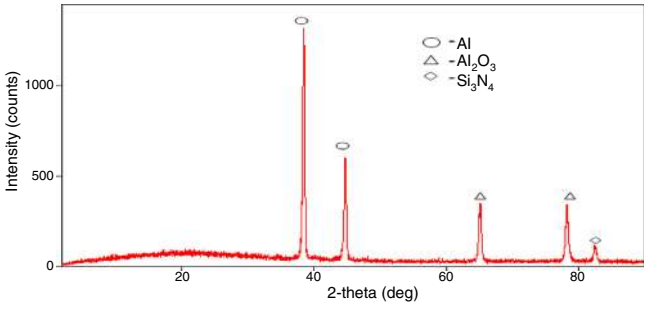

Fig. 4 – XRD result of prepared composite R2.

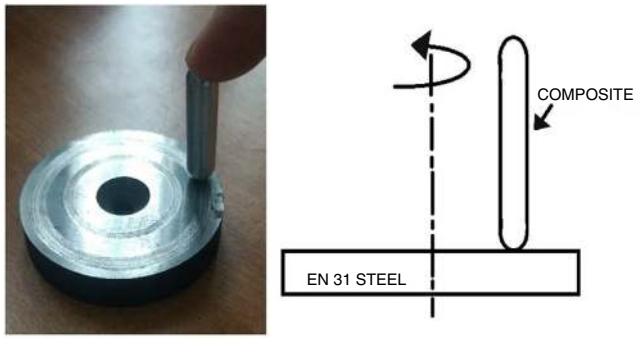

Fig. 5 – Test configuration.

spherical tip were manufactured for the diameter 6 mm and length 45 mm. EN31 steel was used as the disc material. Disc was machined for the diameter of 55 mm and thickness 10 mm. The contact faces of the disc were ground to have average roughness 10 µm. Specimens were cleaned with acetone in order to maintain the accuracy of mass measurement before and after the test. Coefficient of friction with respect to time of wear was recorded by the software integrated with testing machine. Wear rate was calculated by measuring mass loss with the help of electronic weighing machine accompanied 1 mg accuracy. Test configuration is shown in Fig. 5. Five experiments were conducted in each case and the variability of results was accounted.

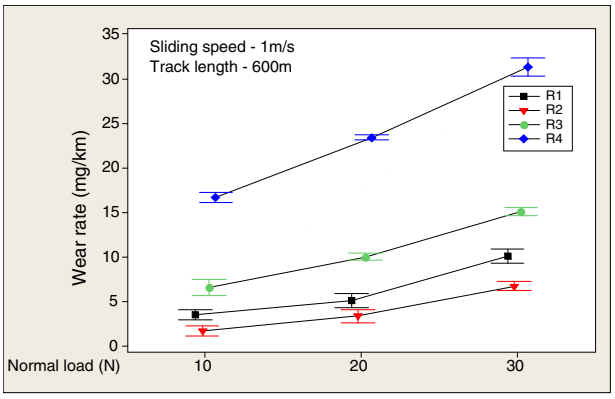

Fig. 6 – Representation of wear rate of composites for low category.

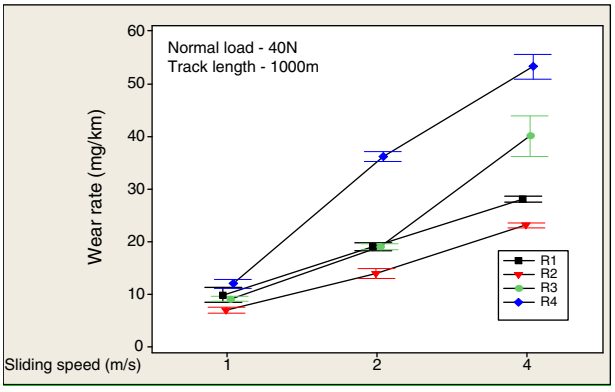

Fig. 7 – Representation of wear rate of composites for high category.

Out of the analysis results of wear rate and average coefficient of friction in all the categories of test, one specimen from each cast was selected for further study on subsurface changes in the composite due to wear. Electric discharge machining (EDM) was carried out to cut the specimens longitudinally. Vickers hardness test was conducted to determine the micro hardness variation in the longitudinal direction from the edge of worn out surface in five different spots along the axis. The distance between the indentations was maintained as 0.5 mm. Test load was given as 0.5 kg and dwell period was set for 10 s.

FESEM and EDS analyses were conducted on worn out surfaces to analyze the nature of wear mechanism in each composite. FESEM images were also taken on the longitudinal cut sections to find out the subsurface deformations due to wear.

3. Results and discussion

3.1. *Influence of premixed reinforcement in wear rate*

Wear rate of the prepared composites in low and high category of wear is represented in Figs. 6 and 7 respectively. As there was no considerable difference in densities of prepared composites, mass loss was used to define the wear rate. Wear rate of composites were increased when normal load was increased as expected. Composites with Al powder premixed reinforcement have shown accountable divergence in wear rate than composites with unmixed reinforcement. Maximum of 15 mg/km was observed with premixed reinforcement 3, which was nearly two times lesser than unmixed reinforcement 4 (31.66 mg/km) at 30 N normal load. The presence of Si_3N_4 nanoparticle in composite has reduced the wear rate than the reinforcement with the only presence of alumina and graphite. Wear rate was reduced when the volume of Si_3N_4 nanoparticles increased in the blend of reinforcement. This is attributed to the dispersion and strong interfacial bonding established between fine nano-sized particles and matrix. High chance of fine sized particle pull out from matrix as discussed in Ref. [12] was controlled by the premixing the reinforcement with Al powder. Wear rate of reinforcement 3 was comparatively lower than reinforcement 4. This is characterized by the premixing of Al_2O_3 and graphite with Al powder which stopped the pull out of Al_2O_3 particles from the matrix. The increment of wear rate from 20 to 30 N normal loads is slightly greater than 10–20 N normal load in all the reinforcement. This shows that the increment in normal load increases the shear stress in the contact surfaces which lead to the rise in wear.

In case of high category, wear rate increased as the sliding speed increases. Severe wear was observed with reinforcement 4. This may be due to the rise of friction in tribosystem at high sliding speed which increases the temperature to cause thermal softening. Wear rate increased as thermal softening reduced the shear strength of the material [4]. Weak interfacial bonding may also be another reason as reinforcement 4 was not premixed with Al. At low sliding speeds (i.e. 1 m/s and 2 m/s), reinforcement 1 and 3 behaved very closely for the wear conditions, whereas, at high sliding speed (i.e. 4 m/s) nanoparticle reinforced composite performed better than micron particle composite. Further, reinforcement 2 with large volume of Si_3N_4 has shown least wear rate in high category as well. This strongly supports the influence of Si_3N_4 nanoparticle in controlling the particle pull out during wear.

3.2. *Effect of premixed reinforcement in coefficient of friction*

Average COF of the composites at low and high category are shown in Figs. 8 and 9. In case of low category, one can witness the reduction in coefficient of friction as the normal load increases in composites with premixed reinforcements. From the graph, one can notice the low average friction of nanocomposites. This is attributed to the presence of Si_3N_4 nanoparticle in reinforcement which premixed the hard Al_2O_3 flakes and reduced the direct contact of composite with counter surface. This effect was further extended in reinforcement 2 with larger amount of Si_3N_4. The composite with reinforcement 3 showed higher friction than other composites. This is due to Al_2O_3 flakes strongly bonded with the matrix as they were premixed with Al powders and they cut the counterface which increases the coefficient of friction. It was witnessed that the reinforcement 4 exhibited lower friction than reinforcement 3. This is predicted with the Al_2O_3 flakes in reinforcement 4 which were unmixed, could not establish the bonding properly

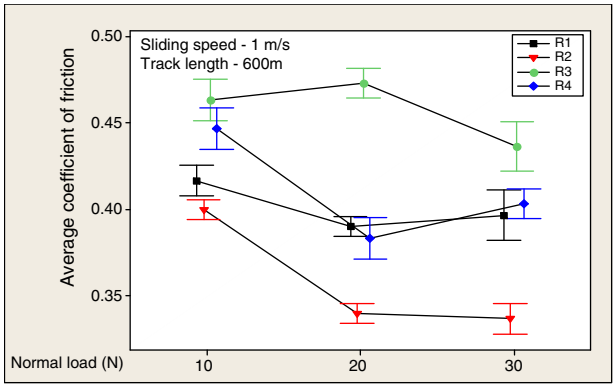

Fig. 8 – Representation of average COF of composites for low category.

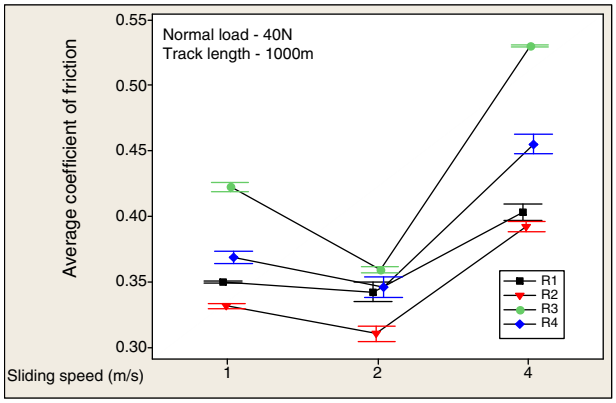

Fig. 9 – Representation of average COF of composites for high category.

with the matrix as a result of that they were pulled out during wear. Even though the reinforcement 4 illustrated lesser average coefficient of friction than reinforcement 3, the wear rate results were opposite between reinforcement 3 and 4. The reason for this conflict is due to the formation of transition layer in between mating surfaces as the strongly bonded alumina in R3 cut the counter face material. The cut out particles forms a mechanically mixed layer (MML) which reduces the wear rate of the material.

On continuing the behaviour in high category, while increasing the sliding speed from 1 to 2 m/s, there is a reduction in average COF. This is attributed to the presence of graphite in all the composites which might have acted as lubricant in between mating surfaces. This phenomenon was encouraged further by thermal softening due to the temperature rise in pin material when the sliding speed was increased. This could be very clearly seen from the result of reinforcement 3. At the sliding speed of 4 m/s, the friction was increased. This is because the formed graphite layer was wiped out due to high mechanical action in the interface and the contact was established between the mating materials which enhanced the friction.

3.3. *Worn surface analysis and mechanism of wear*

The FESEM analysis was carried out on worn surfaces and subsurface of four selected composites (one from each cast) which showed exemplary behaviour during wear. The selection was done based on aforementioned results of wear rate and coefficient of friction. The samples were cut according to the dimension required to place them on FESEM equipment. In order to analyze the subsurface of worn out surfaces, the selected samples were cut longitudinally by EDM process. The FESEM images were taken closer to the worn out edge along the subsurface. The EDS analysis was also carried out on the worn out surfaces. The details of selected samples are shown in Table 3.

It was noted from the micrograph of sample S1 that it has the combined effect of adhesive wear and delamination in few spots. This could be because of small clusters formed in the composite R1, which could nucleate cracks in the grain boundary and led to the delamination on worn out surface as shown in Fig. 10(a). Adhesive wear with small, shallow and parallel grooves along with micro cut was noticed with sample S2 worn out surface [13]. The observed micro cuts were not continuous as reported in Ref. [14]. This is due to the larger volume of Si_3N_4 nanoparticles which premixed the larger Al_2O_3 particles to avoid abrasion on counterface. Few wider grooves were also found to show the effect of larger Al_2O_3 particles as depicted in Fig. 10(b). Deep grooves were observed with sample S3 which explains the abrasive wear. This is because of the only presence of larger premixed Al_2O_3 particles in matrix [15]. The reason for the abrasion is that the presence of the strongly bonded Al_2O_3 particles which cut the counterface. This can be witnessed from Fig. 10(c) which shows the protruding particles of Al_2O_3 in the matrix that was smeared off [3]. It was also proved from the EDS analysis in Fig. 11 that there are traces of Fe and Cr elements on the worn out surface of S3. The presence of O in EDS report represents the possibility for the oxidation of cut out Fe metal particles to form of Fe_2O_3 [16]. This mechanically mixed layer reduces the wear rate as it was formed in between the mating surfaces. The MML was wiped out during high sliding speed and normal load conditions of wear test as discussed by Venkataraman and Sundararajan [17]. Abrasive wear with severe plastic deformation was observed with sample S4 as shown in Fig. 10(d) and (e). This is attributed to the exposure of unmixed Al_2O_3 particles to the high stress in the interface of matrix and Al_2O_3 particles. Since the particles are not fused as like Al premixed Al_2O_3, they tend to nucleate the crack in the interface and subsequently the particles are pulled out.

3.4. *Subsurface analysis*

The support moulds were prepared to hold the selected composites and the longitudinal cut section was polished with Al_2O_3 paste on polishing cloths of various grit sizes from coarse to fine. The specimens are shown in Fig. 12. It can be inferred from the results of Vickers micro hardness test represented in Fig. 14, that there was no considerable grain structure changes observed with composite S4 as micro hardness along the axis were almost uniform. The particles pull

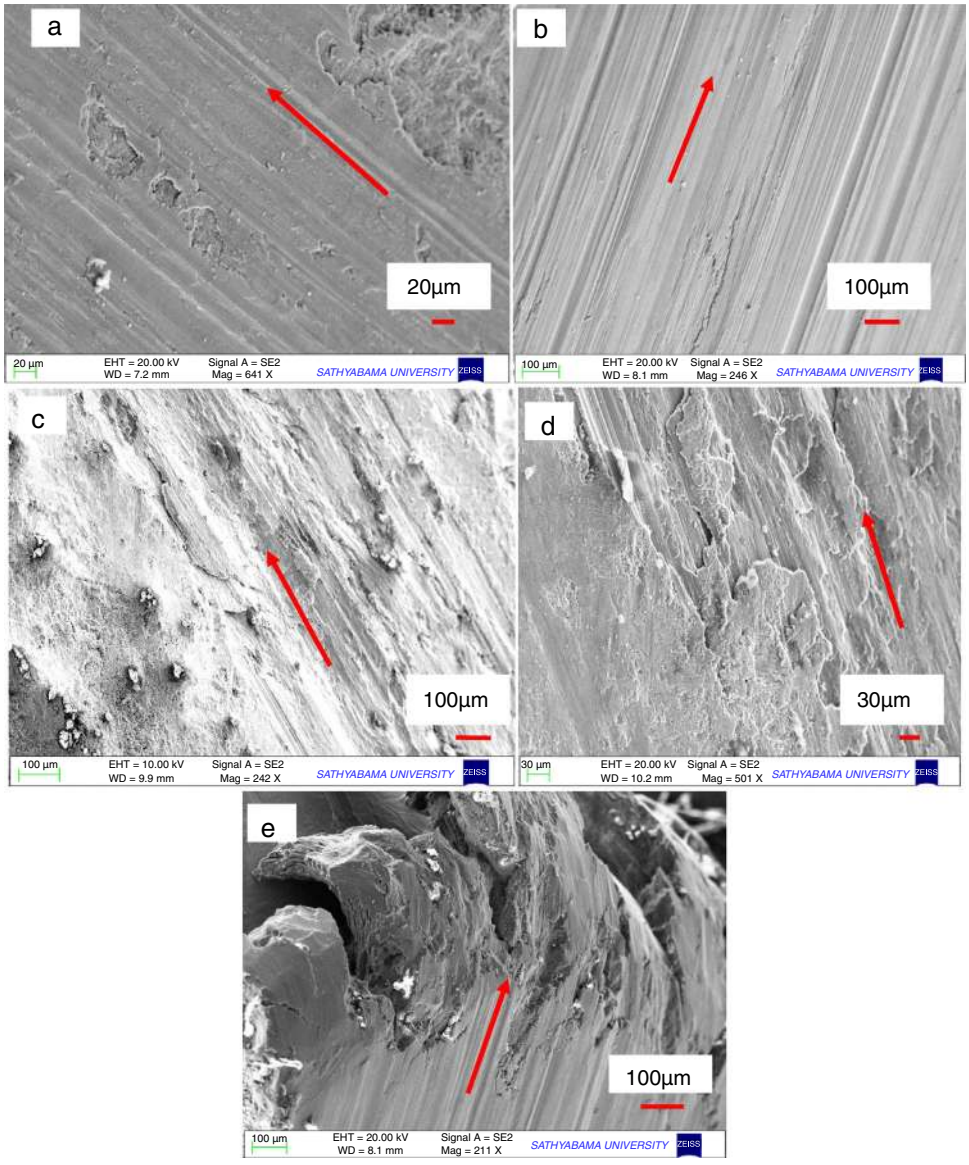

Fig. 10 – FESEM micrographs of worn surfaces (a) adhesive wear and delamination in S1, (b) grooves with micro cut in S2, (c) protruding Al_2O_3 particles in S3 (d) and (e) severe plastic deformation in S4 (arrows indicate sliding direction).

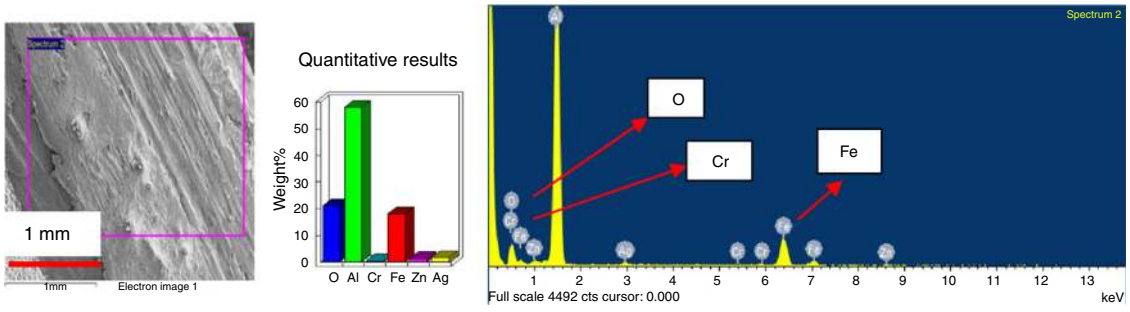

Fig. 11 – Results of EDS of composite S3.

Table 3 – Details of selected sample for morphology.

Sample	Composite	Condition (normal load/sliding speed/track length)	Wear rate (mg/km)	Average COF
S1	Cast 1	40 N/4 m/s/1 km	28	0.35
S2	Cast 2	10 N/1 m/s/0.6 km	1.66	0.40
S3	Cast 3	40 N/2 m/s/1 km	19	0.46
S4	Cast 4	40 N/4 m/s/1 km	53	0.53

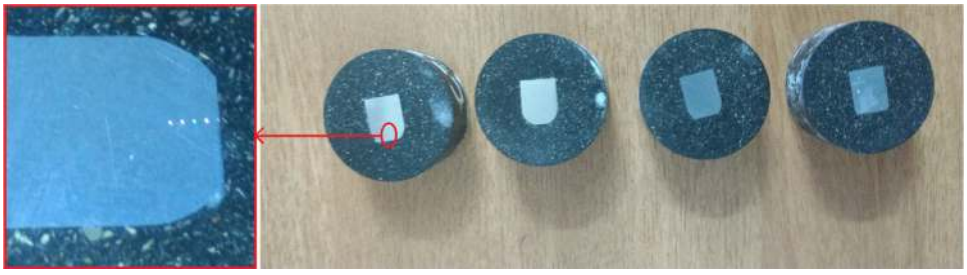

Fig. 12 – Longitudinal cut out specimens for Vickers hardness test.

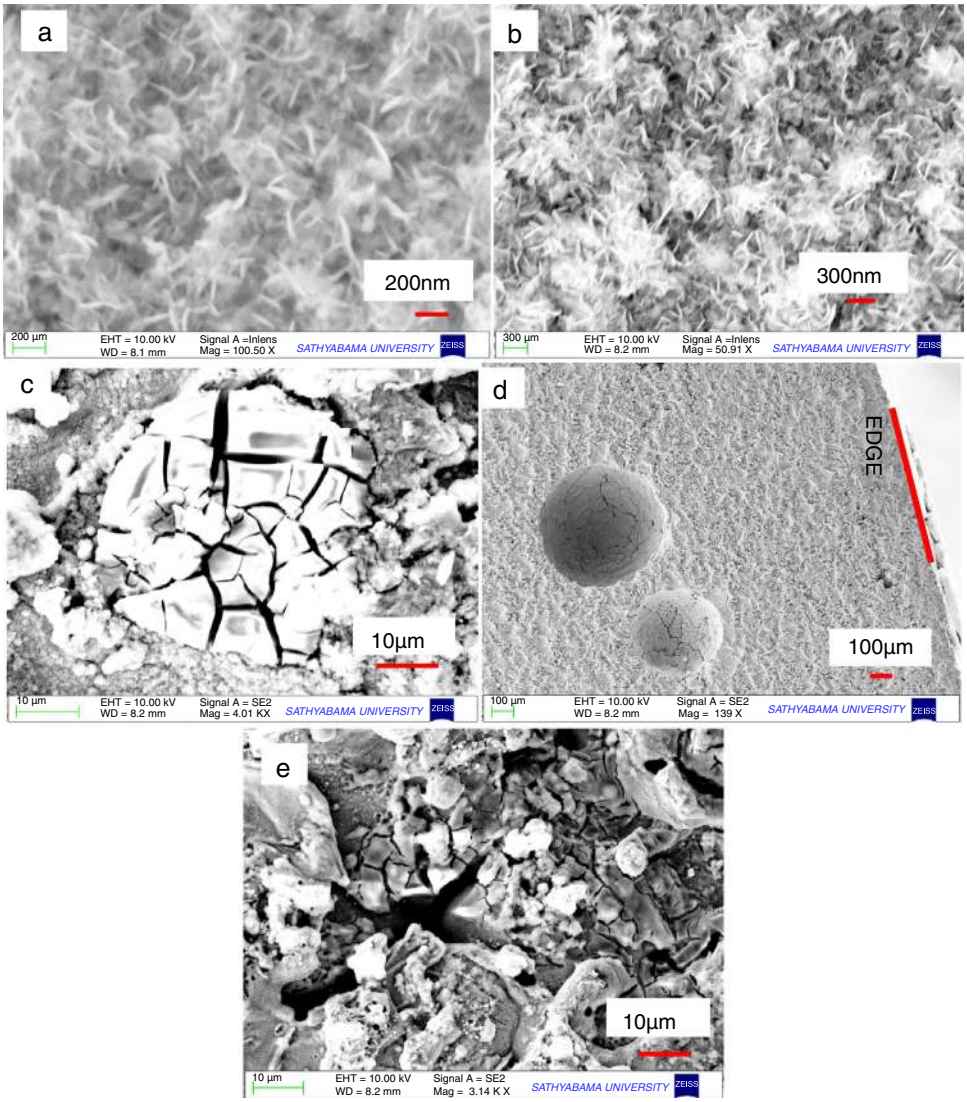

Fig. 13 – Subsurface FESEM micrographs (a) and (b) grain structure refinement in S1 and S2, (c) particle fracture in S4, (d) particle pull out in S4, and (e) porosity in S4.

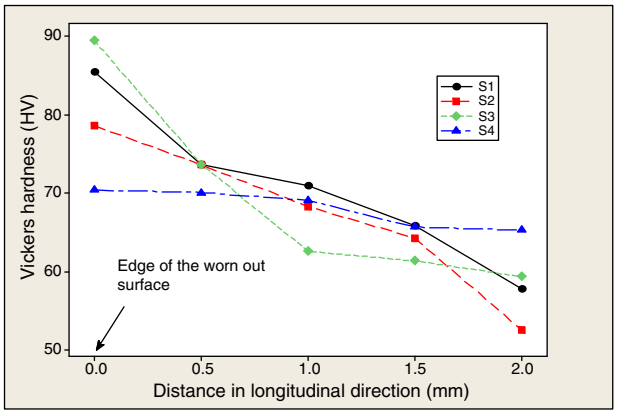

Fig. 14 – Representation of Vickers hardness along the subsurface.

out closer to the worn out edge of S4 was observed as shown in Fig. 13(d). This must have happened during EDM process. This pull out may be attributed to the nucleation of crack in the grain boundary because of stress transferred during wear. This can be identified from the grain structure of the cavity formed by particle pull out in the Fig. 13(d). This kind of pull out was not observed with other selected composites. Particle fracture (Fig. 13c) and pores (Fig. 13e) were also observed in sample S4, which are predicted with the lack of dispersion of unmixed Al_2O_3 particles in the matrix. However, Akbari et al. [8] have expressed that there is no consistency in the effect of porosity on wear properties. The composite sample S3 showed high value of hardness at the worn out edge which strongly support the presence of mechanically mixed layer (MML). The samples S1 and S2 have also showed larger values of hardness at the worn out edge. This could be due to the possibility to form graphite layer on the worn out surface which could further delay the fracture of particles [18]. Similar trend of hardness variation along the axis was observed with composite samples S1, S2 and S3 as shown in Fig. 14. It can be predicted based on the coherence of results variation that the considerable plastic deformation and grain structure changes were happened in these three composites for the length of 1 mm approximately. As the length extends more than 1 mm, the micro hardness reaches the values of as-cast composites. The composites S1 and S2, which contained Si_3N_4 nanoparticles, were observed with grain structure refinement in nanoscale just beneath the worn out surface as shown in Fig. 13(a) and (b). These changes of grain structure might be due to the heat transferred from the worn out surface during friction coupled with mechanical shear force.

4. Conclusion

Hybrid composite of A6061/Al_2O_3/graphite with Si_3N_4 nanoparticles exhibited superior wear properties in both low and high category of wear. The composites with Al premixed reinforcements in A6061 matrix have shown lesser wear rate than composites with unmixed reinforcements. The premixing enhanced the fusion and dispersion of reinforcement particles with matrix. Abrasive wear and the formation of mechanically mixed layer were observed in the composite with the only presence of metal premixed Al_2O_3 and graphite in matrix. The layer was found to be wiped out at high sliding speed. The composites with reinforcement R1 and R2 have shown adhesive wear along with delamination in few spots. The grain structure refinement in nanoscale was also noted just beneath the worn out surface in the composite with Si_3N_4 nanoparticles. Abrasive wear and severe plastic deformation was found to be the wear mechanism in the composite without having the metal premixed reinforcement. Particle pullout, porosity, crack nucleation in grain boundary were also noticed with the unmixed reinforcement composite. The micro hardness test expressed that the premixed reinforcement composites have undergone for considerable plastic deformation and grain structure changes in the subsurface to the depth of 1 mm approximately due to wear.

Conflicts of interest

The authors declare no conflicts of interest.

REFERENCES

[1] Oluwatosin M, Keneth K, Heath L. Aluminium matrix hybrid composites: a review of reinforcement philosophies; mechanical, corrosion and tribological characteristics. Integr Med Res 2015:1–12.
[2] Casellas D, Beltran A, Prado JM, Larson A, Romero A. Microstructural effects on the dry wear resistance of powder metallurgy Al–Si alloys. Wear 2004;257:730–9.
[3] Ko M. Abrasive wear of Al_2O_3 particle reinforced 2024 aluminium alloy composites fabricated by vortex method. Composites A 2006;37:457–64.
[4] Abouelmagd G. Hot deformation and wear resistance of P/M aluminium metal matrix composites. J Mater Process Technol 2004;156:1395–401.
[5] Baradeswaran A, Perumal AE. Study on mechanical and wear properties of Al 7075/Al_2O_3/graphite hybrid composites. Composites B 2014;56:464–71.
[6] Fellah M, Abdul M, Labaiz M, Assala O, Iost A. Sliding friction and wear performance of the nano-bioceramic α-Al_2O_3 prepared by high energy milling. Tribiol Int 2015;91:151–9.
[7] Sahu K, Rana RS, Purohit R, Koli DK, Rajpurohit SS, Singh M. Wear behavior and micro-structural study of Al/Al_2O_3 nano-composites before and after heat treatment. Mater Today Proc 2015;2(4–5):1892–900.
[8] Akbari MK, Baharvandi HR, Mirzaee O. Nano-sized aluminum oxide reinforced commercial casting A356 alloy matrix: evaluation of hardness, wear resistance and compressive strength focusing on particle distribution in aluminum matrix. Composites B 2013;52:262–8.
[9] Wang SR. Microstructure and fracture characteristic of Mg–Al–Zn–Si_3N_4 composites. Theor Appl Fract Mech 2006;46:57–69.
[10] Bindumadhavan PN, Wah HK, Prabhakar O. Dual particle size (DPS) composites: effect on wear and mechanical properties of particulate metal matrix composites. Wear 2001;248:112–20.
[11] Hariharasakthisudhan P, Jose S. Influence of metal powder premixing on mechanical behavior of dual reinforcement (Al_2O_3 (mm)/Si_3N_4 (nm)) in AA6061 matrix. J Alloys Compd 2018;731:100–10.

[12] Kumar S, Balasubramanian V. Developing a mathematical model to evaluate wear rate of AA7075/SiCp powder metallurgy composites. Wear 2008;264:1026–34.
[13] Yang LJ. The transient and steady wear coefficients of A6061 aluminium alloy reinforced with alumina particles. Compos Sci Technol 2003;63:575–83.
[14] Jun D, Yao-Hui L, Si-Rong Y, Wen-Fang L. Dry sliding friction and wear properties of Al_2O_3 and carbon short fibres reinforced Al–12Si alloy hybrid composites. Wear 2004;257:930–40.
[15] Zhang Z, Li X, Almandoz E, García G, Dong H. Tribology international sliding friction and wear behaviour of titanium-zirconium-molybdenum (TZM) alloy against Al_2O_3 and Si_3N_4 balls under several environments and temperatures. Tribiol Int 2016;September:1.
[16] Sharifi EM, Karimzadeh F. Wear behavior of aluminum matrix hybrid nanocomposites fabricated by powder metallurgy. Wear 2011;271(7–8):1072–9.
[17] Venkataraman B, Sundararajan G. Correlation between the characteristics of the mechanically mixed layer and wear behaviour of aluminium, Al-7075 alloy and Al-MMCs. Wear 2000;245:22–38.
[18] Babu JSS, Kang CG, Kim HH. Dry sliding wear behavior of aluminum based hybrid composites with graphite nanofiber–alumina fiber. Mater Des 2011;32(7):3920–5.